Spring 5-2020

Characterization of ncf1 Mutants in a Zebrafish Model of Innate Immune Function with Human Influenza A Virus Infection

Lily Charpentier

CHARACTERIZATION OF *NCF1* MUTANTS IN A ZEBRAFISH MODEL OF INNATE IMMUNE FUNCTION WITH HUMAN INFLUENZA A VIRUS INFECTION

by

Lily Charpentier

A Thesis Submitted to Partial Fulfillment
of the Requirements for a Degree with Honors
(Biochemistry)

The Honors College

The University of Maine

May 2020

Advisory Committee:

Benjamin L. King, Assistant Professor of Bioinformatics, Advisor
Edward Bernard, Lecturer & Undergraduate Coordinator of Molecular & Biomedical Sciences
R.W. Estela, Honors Preceptor
Sally D. Molloy, Assistant Professor of Genomics
Robert Wheeler, Associate Professor of Microbiology

ABSTRACT

Seasonal influenza A virus (IAV) infections and their associated respiratory diseases are the cause of an estimated 650,000 deaths each year, according to the World Health Organization. The zebrafish (*Danio rerio*) is a powerful vertebrate model to study innate immune function and host-pathogen interactions as the function of neutrophils and other phagocytes can be characterized *in vivo*. Preliminary studies have shown an increase in neutrophil respiratory burst activity to eliminate the invading pathogen, yet little is known of all of the mechanisms involved in neutrophil function. The NADPH oxidase complex, of which neutrophil cytosolic factor 1 (Ncf1) is a key component, regulates reactive oxygen species (ROS) to control neutrophil response to viral infection. Although necessary to fight infection, this elicits a hyperinflammatory response that can damage the infected host epithelial tissue, leaving high-risk individuals with increased mortality rates.

Our hypothesis is that a fully functional Ncf1 protein is required for neutrophil function, but morpholino knockdown of the gene will limit the amount of damaging ROS hyperinflammation in host tissue. Our preliminary studies of systemic IAV infected embryos indicate that the survival of *ncf1* morphants was increased compared to standard morphant control groups. Fluorescence confocal imaging and $TCID_{50}$ assays reveal a decreased viral burden in *ncf1* morphant groups compared to control morphant groups over a span of 96 hours post-infection. Finally, qRT-PCR studies assay the expression of *nrf2*, *mxa*, and *cxcl8b* revealing decreased expression of each gene in *ncf1* morphants compared to controls. These studies aim to increase our understanding of neutrophil function that may eventually lead to new therapies for treating IAV infection.

ACKNOWLEDGEMENTS

I would like to thank my advisor Dr. Benjamin King and my graduate student mentor Brandy Soos for all of their guidance and support during this thesis process. I would also like to thank the rest of the King lab and my committee members: Dr. Sally Molloy, Dr. Robert Wheeler, Dr. Edward Bernard, and RW Estela.

TABLE OF CONTENTS

LIST OF FIGURES

INTRODUCTION

The Impact of Influenza A Virus (IAV)

Seasonal influenza infections and their associated respiratory diseases are the cause of an estimated 650,000 deaths each year, according to the World Health Organization. Most infected individuals recover within a week of symptom onset. However, high-risk individuals—such as the elderly, pregnant women, and infants—are susceptible to the systemic spread of IAV, causing severe illness or death [1]. Since 1889, six influenza pandemics have plagued the Northern Hemisphere, the most recent being a deadly outbreak of influenza A (H1N1)pdm09 virus in 2009 [2]. The 2009 pandemic alone resulted in over 60.8 million cases and about 12,500 deaths in the United States [3]. Seasonal flu vaccines are helpful in diminishing the spread of infection, but developing effective vaccines requires accurate prediction of which strains will be most prevalent in advance of each year's flu season. Antigenic drift of the virus' genome makes yearly vaccine design difficult and the risk of pandemics high, highlighting a clear need for alternative therapies.

Influenza viruses belong to the *Orthomyxoviridae* family and can be organized into four different types: A, B, C, and D [4]. This categorization is derived from antigenic differences between the virus' nucleoproteins and matrix M1 proteins, as well as differences in viral reassortment [5]. Influenza A, B, and C viruses each have the ability to infect humans, with A and B strains acting as the main causes for seasonal outbreaks [4].

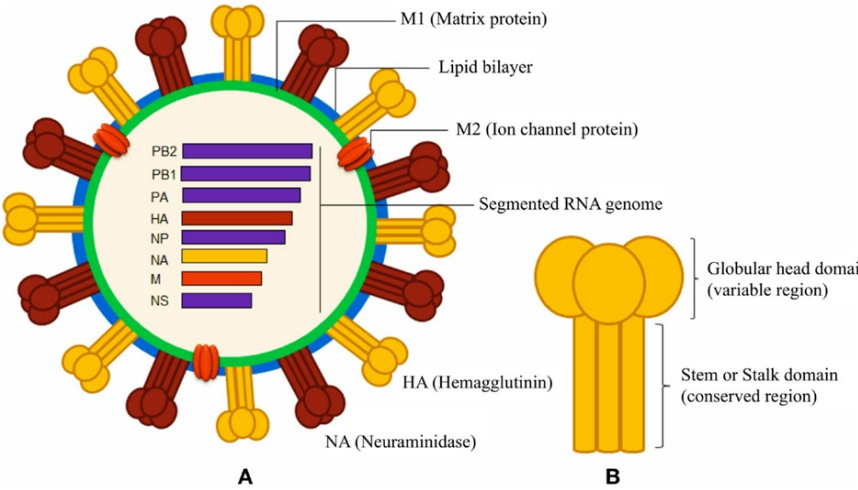

Fig 1. Structure of IAV. A) The IAV genome encodes for the M2 ion channel, neuraminidase, and hemagglutinin envelope proteins along with various nonstructural proteins. B) Hemagluttanin is a homotrimeric protein [6].

Each type of influenza virus can be further classified by its surface neuraminidase (NA) and hemagglutinin (HA) proteins (**Fig. 1**). NA is responsible for cleaving sialic acid linkages of host cell interior glycoproteins. This allows the newly replicated virus to escape the host. HA is used for the recognition and binding of these sialic acid linkages. Currently, 18 HA and 11 NA subtypes have been identified for IAV. Within these subtypes, humans are affected by H1, H2, or H3, and N1 or N2 [7]. Large changes in genome sequence caused by genetic reassortment between animal and human HA subtypes result in an antigenic shift. Although rare, this results in an entirely new strain and pandemic. Such was the case of the 2009 (H1N1)pdm09 swine flu [7]. Alternatively, antigenic drift of these subtypes occurs when singular point mutations minorly alter these surface proteins of influenza, allowing for it to evade recognition by the immune system. With this ability, one strain of IAV can cause recurrent outbreaks throughout a population through constant change in its surface protein presentation. The most prevalent seasonal outbreak strains of IAV are H1N1 and H3N2 subtypes [4]. Due to the ever-changing

nature of IAV, it is imperative to develop novel treatments and therapies against the pathogen.

The Innate Immune Response

When infected by a pathogen, humans rely on two immune responses: The innate and the adaptive response. The innate immune response is conserved within all plant and animal species, while the adaptive immune system is not. As a rapid and nonspecific response, the innate immune system acts as the first responder to infection. It encompasses not only physical and chemical barriers to disease, such as the skin and sweat pH in humans, but also cellular responses [8]. When invading pathogens bypass an animal's physical barriers, the innate immune system will employ proinflammatory cytokine signaling to sites of infection, recruiting phagocytic cells. Pattern recognition receptors (PRRs) are used by innate immune cells in order to recognize highly conserved structures on the outside of microbial species. These structures are called pathogen-associated molecular patterns (PAMPs) [9]. The recognition of specific PAMPs allows the immune system to not only differentiate invading cells from the host's own cells, but it also triggers pathogen-specific cytokine signaling. Within minutes of recognition, cellular signaling cascades cause the upregulation of proinflammatory and cytokine signaling to further recruit innate immune phagocytes to rid the host of the pathogen.

As part of the innate immune response, phagocytic cells known as neutrophils are some of the first responding cells to pathogen invasion. This occurs in a rapid succession of events. First, neutrophils are recruited from the bone marrow, followed by accelerated hematopoiesis to generate new blood cells. Next, the neutrophils will relocate to the

host's bloodstream and marginate along vasculature walls proximal to the site of infection. Finally, through diapedesis, the neutrophils will migrate out of the vasculature towards the infection site [10]. At this point, the neutrophils will be able to interact with and phagocytose the invading pathogen.

The neutrophil response to IAV follows this same process. During phagocytosis, neutrophils will utilize the production of toxic oxygen metabolites to fight infection through a process known as respiratory burst. Although necessary to clear invading pathogens, this elicits a hyperinflammatory response that can damage the infected host epithelial tissue, leaving high-risk individuals with increased mortality rates [11]. This damage is, in part, due to reactive oxygen species (ROS) generated by neutrophils near virus-infected cells. ROS are a group of highly reactive molecules that are mainly produced by phagocytes [12, 13]. At low concentrations, ROS can act as signaling molecules, but at a high concentration have the power to oxidize proteins and lipid components of cells, causing tissue and DNA damage [14]. ROS are generated by the NOX2 NADPH oxidase complex, of which the neutrophil cytosolic factor 1 (*ncf1*) gene encodes a key component.

The NOX2 NADPH Oxidase Complex and ncf1

In order to produce ROS, neutrophils utilize the NOX2 NADPH oxidase complex. There are seven members of the NOX family, including NOX1-5 and DUOX1 and 2. The NOX2 NADPH oxidase complex is the predominant ROS producer in humans [15]. This complex consists of a Nox2 transmembrane electron carrier that is stabilized and activated by four subunits (p22, p47, p67, and Rac2) (**Fig. 2**) [12]. Nox2, also known as

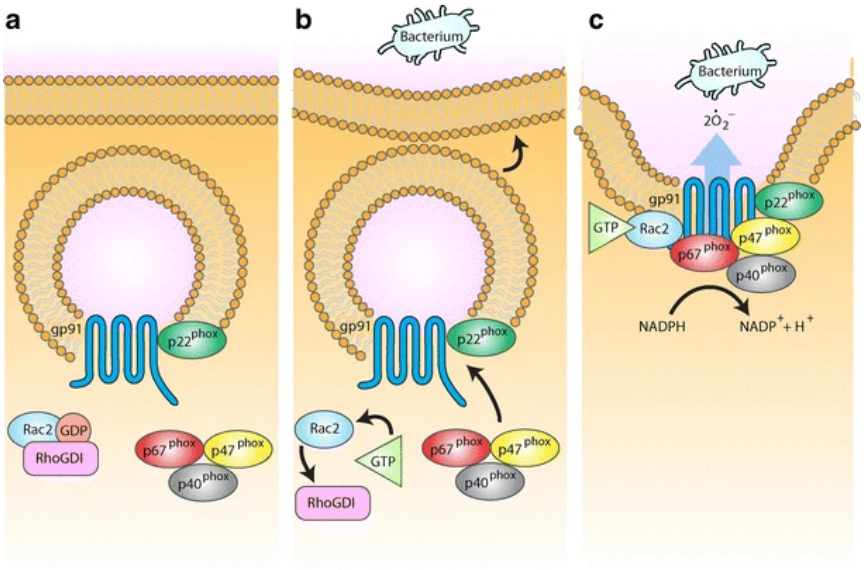

Fig. 2 NOX2 NADPH oxidase complex. A) Complex in resting stage. B) Once activated, regulatory subunits migrate to the membrane. C) The complex produces ROS to fight an invading pathogen [13].

the cytochrome b-245 heavy chain, is the phagosome membrane-bound component of the NADPH oxidase complex and consists of the functional transmembrane heterodimers gp91^{phox} and p22^{phox} [13]. While dormant, Nox2 will remain within intracellular vesicle membranes, while the other components remain trimerized in the cytosol [13].

Once activated during phagocytosis, GDP-Rac2 is converted to GTP-Rac2, which allows for it to be translocated to the phagosome membrane from the cytosol, along with Nox2 from the vesicle membrane [16]. At the same time, the p47^{phox} subunit (which is encoded by the *ncf1* gene) undergoes a conformational change caused by phosphorylation. This exposes two SRC-homology 3 regions that can interact with a proline-rich motif on the p22^{phox} subunit of Nox2 [13]. Additional Phox homology domains exposed on p47^{phox} can bind to phosphatidylinositol 3-phosphate (PI(3)P) and PI(3,4)P2, which are produced at the plasma membrane during phagocytosis. This allows for further stabilization with Nox2 at the plasma membrane [15]. Once the complex is assembled, the gp91^{phox} subunit converts NADPH to NADP+, freeing two electrons to be

transported through the Nox2 complex into the phagosome. There, they react with molecular oxygen to create ROS [12].

The NOX2 NADPH oxidase complex may have many implications in neutrophil antiviral and antioxidant immune responses to infection. Specific subunits of this complex may prove to be key modulators of these functions. $p47^{phox}$, now commonly known as Ncf1, is a key activator of the NOX2 oxidase complex. Knockdown of *ncf1* expression has been shown to not only hinder an organism's ability to produce superoxide anions but also creates a loss of phagocyte recruitment to sites of infection [17]. Not only does it play an integral role in the production of pathogen-fighting ROS, but it can act as a key regulator of the antioxidant response to ROS. For example, to counteract the overproduction of tissue-damaging ROS Ncf1 activates Nrf2 (an antioxidant transcription factor) and therefore increases antioxidant expression. Previous studies have shown that a decrease of *ncf1* expression decreases Nrf2 activation, while the other NOX2 subunits have no effect [18]. Ncf1 is a novel target for alternative IAV therapies, as it plays a critical role in neutrophil function.

The Zebrafish Model

The use of *in vivo* animal models in biomedical research allows for the study of the pathogenesis of human diseases at both the cellular and organismal levels. Being able to observe the effects of pathogens in organisms allows for the characterization of their effects on living systems, a distinct advantage over the use of *in vitro* cell or tissue culture. Mammalian models, such as mice and rats, are commonly used in biomedical research due to their genetic and anatomical similarities to humans. However, they pose

financial and physical restraints such as long gestation periods [19]. Invertebrate models cost less to maintain, but lack many organ systems to model disease pathology.

The zebrafish (*Danio rerio*) is a powerful vertebrate model to study human disease. Zebrafish have been used to model embryonic development since the 1930s [19]. Their optical clarity and ease of cellular manipulation are useful for biological research. The model was further developed in the 1980s with the advent of genetic techniques such as mutagenesis, making zebrafish a standard model in developmental biology. With high fecundity of over 100 embryos per clutch and ease of genetic manipulation through either morpholino (MO) gene knockdown (KD), or transgenesis, such as CRISPR knockout (KO), zebrafish encompass the ease of use. Like other vertebrate models, zebrafish share high (70%) genetic and organ system homology to humans, making them ideal for modeling infection (**Fig. 3**) [19].

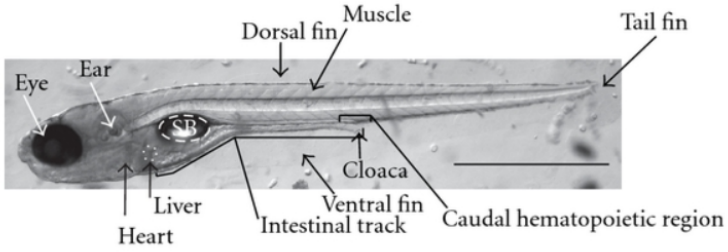

Fig. 3 Zebrafish anatomy taken at 6 days post-fertilization (dpf) with brightfield microscopy. Scale bar is 1 mm [20].

Zebrafish are well-established models for infectious disease, especially for the innate immune response. They share high similarity with the human innate immune system, containing many of the same responding cell types including neutrophils, macrophages, and Natural Killer cells. Cytokine signaling pathways are also highly conserved [20]. The zebrafish innate immune system is fully functional by 48 hours post-fertilization (hpf), allowing researchers to observe immune cell response during early larval development. Furthermore, their adaptive immunity does not develop until 4 – 6

weeks post-fertilization, allowing for no interference with the innate immune response [20].

Previously, the Dr. Carol Kim lab at the University of Maine has established the zebrafish as a novel model for IAV infection [21]. Not only do cells in the zebrafish have α-2,6 sialic acid linkages on the surface required for human IAV hemagglutinin proteins to bind—which other animal models, such as mice, may lack [22]—, but they also display tissue-destruction pathology similar to that of IAV infected human patients [21]. Zebrafish also exhibit characteristic signs of IAV infection, such as edema and hyperinflammation (**Fig. 4**). Influenza infection can cause acute respiratory distress syndrome (ARDS). One of the driving features in the pathogenesis of ARDS is the accumulation of fluid in the alveoli, which causes severe pulmonary edema. In zebrafish, a similar effect is characterized by a pericardial effusion from the yolk sac.

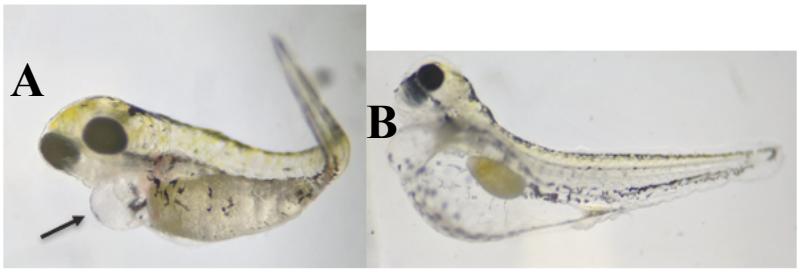

Fig. 4 Zebrafish 3 dpf exhibiting edema and hyperinflammation. A) Edema exhibited by a pericardial effusion, indicated by the black arrow.
B) Hyperinflammatory response.

Furthermore, zebrafish larvae are relatively transparent, allowing for observation and imaging of fluorescent IAV strains and the resulting neutrophil response. Zebrafish have also been verified as effective models of *Pseudomonas aeruginosa* infection by the Kim lab, and fungal *Candida albicans* infection by the Dr. Robert Wheeler lab of the University of Maine [17].

Although the zebrafish model has its advantages, it also has disadvantages. As a new model, relative to well-established models such as the mouse, zebrafish have fewer

available mutant and transgenic strains, as well as fewer known antibodies for use [20]. They also have various duplicate genes, which makes forward-reverse genetic manipulation difficult [20]. Finally, they thrive in markedly different conditions than humans do. They require an environment with high salinity, as well as a temperature between 25 – 31°C for adult fish and 25 – 33°C for embryos [23]. Each is lower than the ideal human temperature of 37°C [19].

Despite its disadvantages, the zebrafish model is well suited for IAV studies. Other animal models, such as mice, ferrets, and guinea pigs have been used with IAV infection. For example, ferrets also have α-2,6 sialic acid linkages on the surface of cells, allowing human IAV to effectively infect cells [22]. They are able to provide insight into not only an immune response, but also how IAV affects organ systems similar to that of a human. However, much like other models, zebrafish also display tissue-destruction pathology similar to that of IAV infected human patients [21]. The transparency of zebrafish larvae is an advantage over other models, as this allows for observation and imaging of fluorescent IAV strains and the resulting neutrophil response *in vivo* of the entire organism, without the need of tissue sample removal. The innate immune response can also be observed unaffected by the adaptive response until about a month post fertilization. Finally, the high fecundity allows for extensive experimentation. Ferrets for example, generally have fewer than ten kits per litter, while zebrafish have about 100 embryos per clutch. Zebrafish require less space, food, and resources to rear than ferrets and other mammalian models, allowing for more specimens to study.

The zebrafish innate immune response is a well-known model for the human response, but it is not fully characterized. The exact mechanisms and signaling pathways

involved in neutrophil chemotaxis and general response to influenza A infection are not fully understood. This study aims to further characterize the role of *ncf1* during the zebrafish innate immune response to IAV infection. The hyperinflammatory response and the NOX oxidase complex can be damaging to host tissue, but it may play a critical role in the response to IAV. As a key activating subunit of NOX2, *ncf1* provides a novel target of study of the modulation of ROS production. Using morpholino KD of *ncf1*, we hope to determine the role of Ncf1 in infection and provide new avenues for future genetic therapies against viral infection and hyperinflammation.

MATERIALS AND METHODS

Zebrafish Care and Maintenance

Embryos were collected at the 1 cell stage from spawning wild-type AB and Tg(*mpx*:GFP) zebrafish. Embryos were stored in 50 mL of egg water (60 mg/L Instant Ocean, Spectrum Brands, Madison, WI) at 33°C.

Microinjection

At the 1 - 8 cell stage (0.5 to 1 hpf), embryos were injected with 1 nL of either standard control, *p53*, or *ncf1* MO (Gene Tools, LLC, Philomath, OR) at concentrations of 100-200 μM/nL. The *ncf1* MO mix contained equal concentrations of E4I4 and translational MO. An additional group was coinjected with both *p53* and *ncf1* MO. Following injections, dead embryos were removed from each group, the egg water replaced, and the fish returned to an incubator and held at 33°C.

For systemic IAV infection at 48 hpf, larvae were dechorionated and anesthetized in 200 mg/L tricaine/egg water solution. Infection groups are separated into live virus, heat-inactivated virus, UV-inactivated virus, and mock infection. Chilled Influenza A/PR/8/34 (H1N1, EID_{50} $5.5x10^4$) in 1X HBSS with phenol red was injected into the duct of Cuvier to cause systemic infections in experimental groups. For mock infection controls, Hank's Balanced Salt Solution (HBSS) with phenol red was injected in the same manner. Systemic injections were in 1 nL doses.

Localized infections to the swimbladder were injected at 96 hpf with mCherry ColorFlu IAV [24]. Mock infection controls were injected with HBSS. Localized injections were administered in 3 consecutive 5 nL doses.

Survival Curves

Following duct of Cuvier injections in 48 hpf embryos, the survival rates of fish in each sample group were measured on a daily basis over a span of 6 days post-infection. Deceased fish were removed from plates at each 24-hour timepoint. The amount alive for the day divided by the total sample at day 0 constitutes the day's survival percentage. Survival curve data and significance were recorded and graphed using GraphPad Prism 8 (GraphPad Software, San Diego, California USA, www.graphpad.com).

$TCID_{50}$

Embryos were injected with either a standard control, *ncf1*, or *ncf1/p53* MO. At 48 hpf, these groups were split into three equal cohorts infected with either live influenza virus, heat-inactivated virus, or HBSS mock infection. Immediately after infection, 6 fish were collected from each group by anesthetizing in 400 mg/L tricaine/egg water solution and suspended in 500 µL RNALater solution before being flash-frozen for future use. Collection was repeated at 24, 48, 72, 96, and 120 hours post-infection (hpi).

Madin-Darby Canine Kidney London line (MDCK-London) cells were grown in T175 flasks in MEM-NCS for use. Cells were then plated into 96-well plates at 50% confluency. For an experimental set of 0-96 hpi time points, a total of 6 plates were plated. MEM-BSA was prepared with 0.5 mg/mL TPCK-Trypsin from 1 mg/mL aliquots 1:2000 and kept chilled.

The frozen fish samples were defrosted, the RNALater solution was removed, and 300 µL of the MEM-BSA/TPCK-Trypsin added to each tube. The fish were homogenized for 4 min. at 4°C. Serial dilutions of the samples were performed with 450

mL MEM-BSA/TPCK-Trypsin media to 50 mL of slurry from 10^{-1} to 10^{-7} for IAV samples and 30 mL of slurry to 270 mL of MEM-BSA/TPCK-Trypsin media for HBSS and heat-inactivated samples.

The MDCK-London cells were then rinsed twice with cold 1x PBS. The serial dilutions were then added in 35 µL to the plated MDCK-London cells in triplicate. The plates were centrifuged for 5-10 minutes at 4°C, 2,000 g. Plates were then placed on a rotator at 4°C for 30 min., tapping in 15 min. intervals. Next, they were transported to a rotator at 33°C for 60 min., with tapping at 10 min. intervals. Once incubation was complete, the media was removed and 100 µL fresh MEM-BSA/TPCK-Trypsin was added to each well. Plates were placed in 37°C incubation for 3-5 days and observed every 24 hours for cytopathic effects. $TCID_{50}$ was determined using the Spearman and Kärber method.

qPCR

Sample groups consisted of standard control or *ncf1* morphant fish, each infected with either live influenza virus or HBSS mock infection. Each treatment group replicate contained 6 fish. Larvae were collected 24 hpi and euthanized in 400 mg/L tricaine/egg water solution and suspended in 125 µL of Trizol before being flash-frozen for future use. RNA was extracted from sample groups using the Zymo Research Micro Prep Kit as per the manufacturer's instructions. Sample concentrations were determined with the ThermoFisher Scientific NanoDrop One and stored in -80°C until needed. cDNA was synthesized from extracted RNA with the NEB ProtoScript II cDNA Synthesis Kit according to the manufacturer's instructions with the oligo dT23 variation.

For each gene of interest, 100 μM forward and reverse oligos (IDT, Iowa City, IA) were added in 5 μL aliquots each to an Eppendorf tube followed by 90 μL of DNase/RNase free water and vortexed. β-actin was used as a known control. A master mix was created for each gene of interest. For each reaction: 5 μL SsoAdvanced Universal SYBR Green Supermi (BioRad, Hercules, CA), 3.5 μL nuclease-free water, and 0.5 μL forward/reverse oligo mixture were combined into a master mix tube. A 96-well plate was labeled for each sample group and replicate. The master mix was added to each sample well in 9 μL volumes. Sample cDNA for the samples and no-RT controls were added to each appropriate plate, vortexing the sample tubes before addition. Once all cDNA has been added, the plate was covered with adhesive film for BioRad qPCR plate, vortexed, and spun in the centrifuge. The plate was placed in a BioRad CFX96 plate and the thermocycler programmed for the following: 10 min. at 95°C; 30 sec. at 95°C, 1 min. at 55°C, 1 min. at 72°C, 40 times; 1 min. at 95°C; 30 sec. at 55°C; 30 sec. at 95°C; Hold.

Imaging

Tg(*mpx*:GFP) zebrafish were infected with *mCherry* ColorFlu IAV (Fukuyama et al, 2015) or HBSS control at 4 dpf. Images were obtained using the Olympus Fluoview 1000 on an Olympus IX-81 inverted microscope at 20X magnification. Samples were mounted in 0.8% agarose solution on a 24-well glass-bottom plate.

RESULTS

Ncf1 Knockdown Results in Significantly Increased Survival of AB Zebrafish

In order to preliminarily gauge the effect *ncf1* knockdown has on zebrafish survival, three replicate survival trials were conducted comparing wild-type (WT), scrambled control morphant, *p53* control morphant, *ncf1* morphant, and *ncf1/p53* morphant groups. Some morpholinos can induce apoptosis in morphants and the *p53* morpholino has been shown to diminish off-target cell death [25]. To study this effect in *ncf1* morphants, a *ncf1/p53* coinjection group is included in the study, as well as a group only injected with *p53* as a control. Embryos from each group were infected with either HBSS or live IAV.

All groups injected with HBSS vehicle control had the same rates of survival (**Fig. 5A**). As expected, the scrambled control and WT morphant groups had similar rates of survival near 60% (**Fig. 5B**). After a 6-day observation period, *ncf1* morphant survival fell to roughly 75% with IAV infection, which is significant compared to the WT and control morphant rates with a *p*-value of 0.0190 by the Log rank (Mantel-Cox) test (**Fig. 5B**). Each treatment group initially consisted of 50 zebrafish and the survival curve performed in triplicate.

p53 morphants had roughly 65% survival after the 6-day period (**Fig. 5C**). It was expected that coinjection of *p53* MO and *ncf1* MO would decrease *ncf1* MO-induced off-target effects. Hypothetically, this would cause the *ncf1*/*p53* coinjection group to have the same, if not slightly increased, survival compared to the *ncf1* MO group. This was not the case, with the *p53* and *ncf1/p53* MO groups having the same rate of survival (**Fig. 5C**).

Although appearing to have a slightly decreased survival rate of 65% compared to *ncf1* MO, the *ncf1/p53* group was not significantly different with a p-value of 0.0775 (**Fig. 5C**). Due to this, the *p53* and *ncf1/p53* groups were excluded from further study.

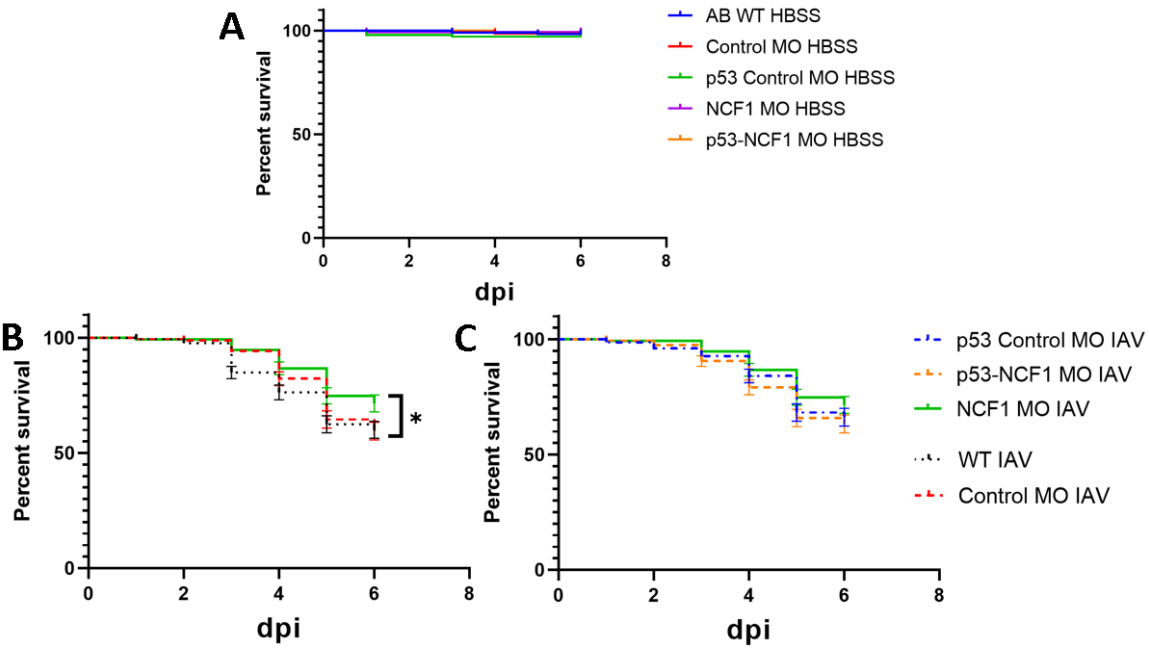

Fig. 5 Survival of IAV or mock challenged zebrafish after morpholino treatment. A) HBSS vehicle control group survival. B) Survival of wild-type, control morpholino, and *ncf1* morpholino IAV infected groups. *ncf1* morphant fish have significantly higher rates of survival than wild-type fish when infected with influenza with a *p*-value of 0.0190. C) Comparison of *p53* morphant, *ncf1/p53* morphant, and *ncf1* morphant survival. IAV infected groups have lower rates of survival than HBSS injected counterparts with a *p*-value of <0.0001.

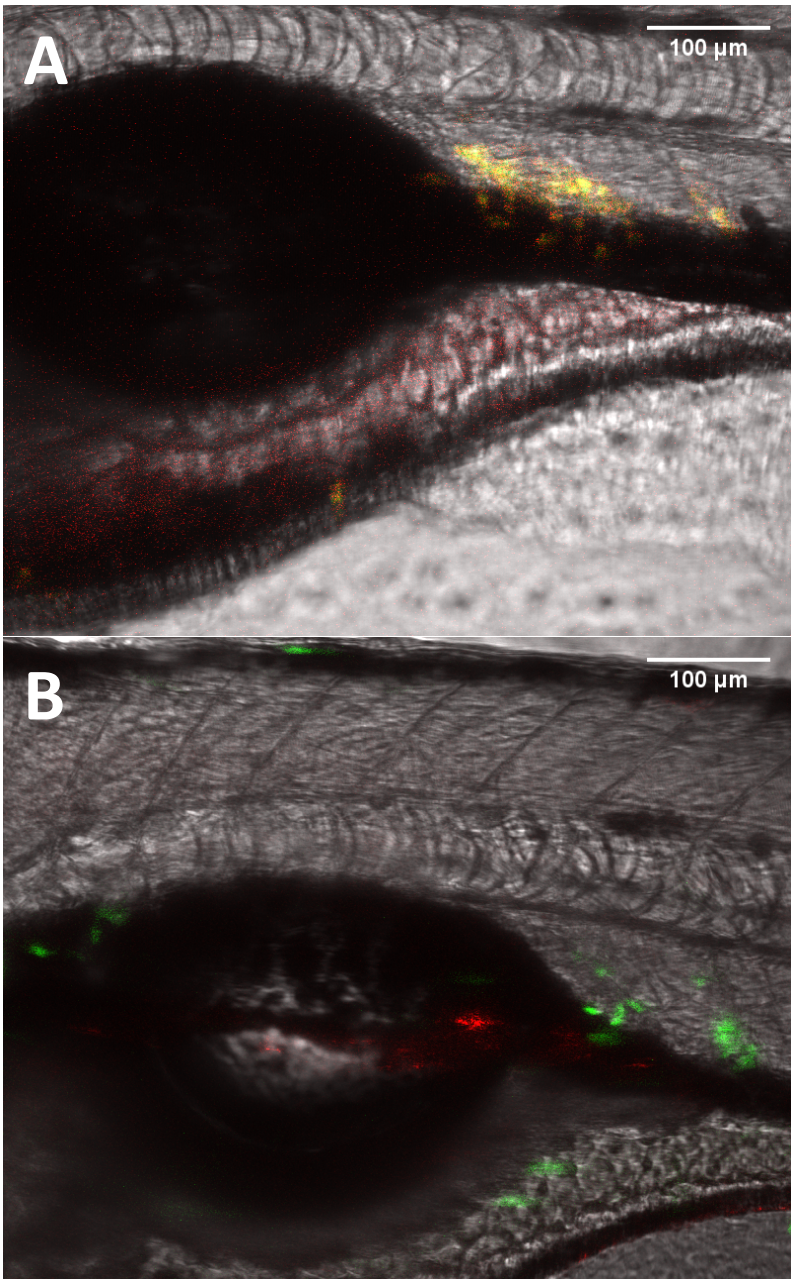

Fig. 6 *ncf1* morphant fish have lowered neutrophil chemotaxis to IAV swimbladder infection than standard control morphants. Fluorescence confocal imaging of Tg(*mpx*:GFP) fish with mCherry color IAV at 48 hpi. Neutrophils are identified by green fluorescence and IAV infection by red fluorescence. A) Scrambled control morphant fish. B) *ncf1* morphant fish.

ncf1 Morphant Fish Have Lowered Neutrophil Chemotaxis to Localized Sites of IAV Infection and Decreased Viral Burden During Systemic Infection Compared to Control Morphants

To qualitatively assess the neutrophil response to infection, fluorescence confocal images were taken of Tg(*mpx*:GFP) zebrafish injected with either scrambled control MO or *ncf1* MO. Fish were infected with red fluorescent mCherry IAV at 72 hpf and imaged at 2 days post-infection. Neutrophils in scrambled control morphants have increased interaction between the virus compared to those of *ncf1* morphant fish, exemplified by the increased amount of yellow in the image (**Fig. 6**).

The Median Tissue Culture Infectious Dose ($TCID_{50}$) is a method to quantify viral titer. It signifies the viral concentration at which 50% of cultured cells within a well plate are inoculated with a dilution of virus. $TCID_{50}$ results yield decreased viral burden in *ncf1* morphants compared to scrambled control morphants by at least a factor of 10 at all time points over a span of 96 hours post infection (**Fig. 7A**). The largest disparity between *ncf1* morphants and controls occurs at 24 hpi, at which viral burden decreases by a factor of 1000 (**Fig**. **7A**). Cytopathic effects were observed as cell rounding and granularity, as well as grouping (**Fig. 7B, 7C, and 7D**).

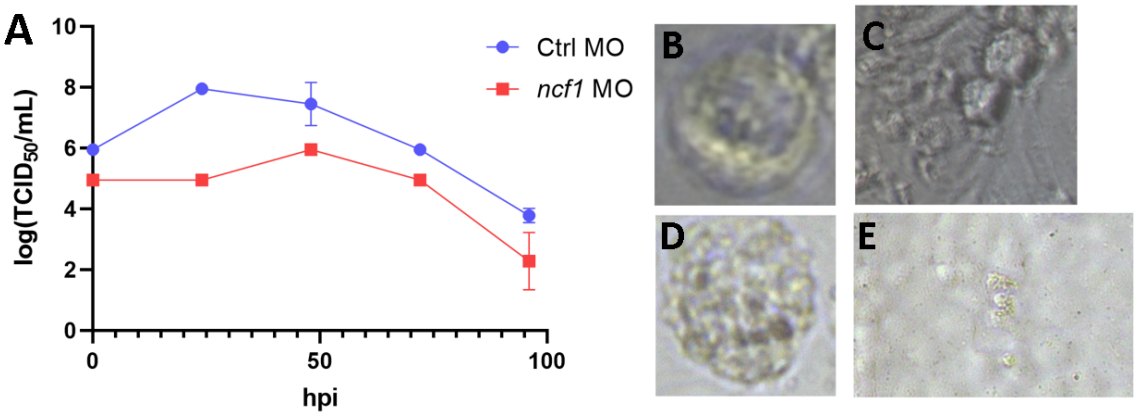

Fig. 7 *ncf1* morphants have decreased viral burden compared to standard control morphants. N = 2. A) Curve of TCID50/mL values over 96 hpi. B) Cell rounding cytopathic effect. C) Cell grouping cytopathic effect. D) Appearance of cytoplasmic inclusion bodies. E) Cells without cytopathic effects.

ncf1 Morphants Exhibit Decreased *nrf2*, *mxa*, and *cxcl8b* Expression Compared to Control Morphants

To gauge gene expression changes in *ncf1* mutants compared to controls at 24 hpi, qRT-PCR was conducted on *nrf2*, *mxa*, and *cxcl8b*. Nrf2 is an important regulator of the zebrafish antioxidant defense against ROS [26]. Mxa, also known as Myxovirus (Influenza) resistance A, is also of interest. Finally, Cxcl8b has been shown to be a regulator of neutrophil migration in zebrafish [27].

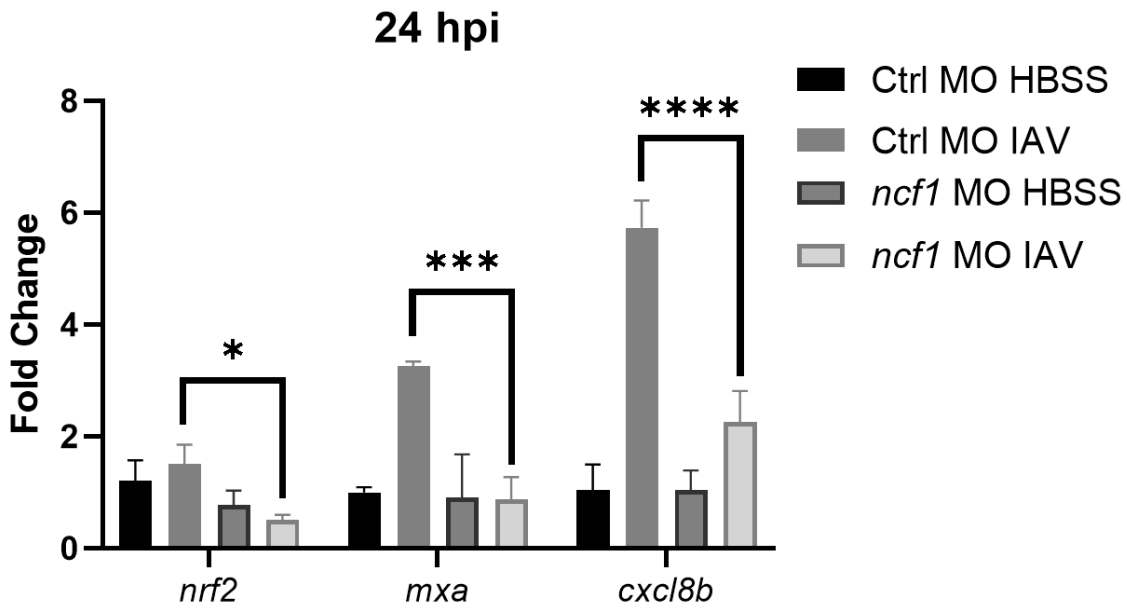

Fig. 8 Relative expression levels of *nrf2*, *mxa*, and *cxcl8b* treated with scrambled control and *ncf1* morpholinos with IAV and mock infection as measured by SYBR Green qRT-PCR. Graphs represent the mean fold change plus or minus standard error. N = 3. Significance between each comparison are *p*-values of 0.0257 (*), 0.0001 (***), and <0.0001 (****), respectively.

With IAV infection *ncf1* morphant fish had decreased expression of each of the three genes compared to their control MO counterparts (**Fig. 8**). This indicates that *ncf1* expression has an impact on the innate antiviral response to IAV.

DISCUSSION

Influenza is responsible for over 650,000 deaths each year globally and 6 pandemics since the late 1800s. In the United States alone, the CDC estimates that IAV causes anywhere between 140,000 to 810,000 hospitalizations per year. High-risk individuals are not only plagued by the virus, but are also burdened by a hyperinflammatory response by their own immune system, which can lead to lung epithelial tissue damage. Mechanisms involved in the innate neutrophil response and hyperinflammation are not fully characterized. Using an *in vivo* zebrafish model, this study aims to characterize the innate immune response to IAV infection with *ncf1* expression knockdown.

The first goal of this study was to characterize the survival of zebrafish with *ncf1* knockdown in response to systemic IAV infection. Compared to infected wild-type fish, *ncf1* morphants had a significantly increased rate of survival after 6 days post-infection (dpi) (**Fig. 5**). The rate of survival was raised from about 55% to 75%, respectively. By inhibiting the ROS production of the NOX2 NADPH oxidase complex through MO knockdown of its key activating subunit, it is possible that the damaging, and lethal, hyperinflammatory response was decreased.

Knockdown of *ncf1* during IAV infection may increase survival due to interference of viral pathways that lead to suppression of antiviral immune responses. Host-pathogen interaction mechanisms involving NOX2 may contribute to the increased survival of *ncf1* morphants compared to controls. These survival findings are consistent with previous IAV studies [28] and observations of patients with chronic granulomatous disease with *NCF1* mutations [29, 30]. Recently, research has indicated that IAV interacts

with the host immune response through Toll-like receptor-7 (TLR7)-dependent signaling to increase NOX2 activity [31]. TLR7 is an essential activator for B-cells and antibody production. NOX2 activation by IAV infection leads to the suppression of antiviral cytokines through the suppression of antibody production. This leads to a lowered ability of the host to clear viral infection and a lowered resistance to re-infection [31]. The impairment of this mechanism used by IAV could possibly lead to increased fish survival. There are likely many antiviral pathways affected by NOX2 activity during infection. Discovering the various mechanistic roles of NOX2/Ncf1 and their subsequent ROS signaling and cytokine pathways could provide novel therapeutic targets against damaging hyperinflammation and IAV infection.

p53 morphants were analyzed as previous studies of other morphants showed off-target effects, which could be reduced with use of a *p53* morpholino [25]. Past research indicates that injecting with *p53* morpholino does not significantly impact the initial survival of zebrafish and embryos are developmentally normal [32]. Due to this, it is expected that the *p53* MO control group survival would not significantly deviate from that of the standard control and WT groups. Although the *p53* MO control group did have increased survival compared to the WT and standard control MO groups, it was not significantly higher. It was also not significant from the *ncf1*/*p53* coinjection group. Morpholino knockdown can be a contributing factor to decreased fish survival. Some morpholinos can induce apoptosis in morphants and the *p53* morpholino has been shown to diminish off-target cell death [25]. In order to limit off-target effects and create accurate survival curves, another sample group was coinjected with both *ncf1* and *p53* MO. However, this did not prove to increase fish survival. Coinjecting *p53* with *ncf1*

decreased survival by roughly 10% from *ncf1* morpholino alone and was not significant from the aforementioned control groups (**Fig. 5**). Apoptosis is required to rid an organism of defective cells. Although the *p53* morpholino was not expected to decrease survival, it is possible that by limiting apoptosis, there was increased stress and burden on the zebrafish, leading to lowered survival.

The second goal of this study aimed to characterize the general neutrophil response and viral burden of IAV infection in *ncf1* morphant fish. The Kim lab has established the zebrafish swimbladder as a site for localized IAV infection. After infecting recombinant fluorescent Tg(*mpx*:GFP) fish at 4 dpf with mCherry color flu, confocal images were taken. This allowed us to qualitatively assess both neutrophil migration and interaction with IAV, as well as clearance of IAV over time. As expected, scrambled control morphant fish have a larger active neutrophil response to infection, with a high amount of interaction with the pathogen compared to their *ncf1* morphant counterparts (**Fig. 6**). Surprisingly, even though *ncf1* morphant fish had lowered neutrophil chemotaxis to the site of infection, shown by an increase of yellow indicating neutrophil-pathogen interaction in control morphants compared to *ncf1* morphants, they also appeared to have a lower viral burden (**Fig. 7**). This brings to question the involvement of other phagocytic cells in the absence of a neutrophil response, namely macrophages. In the future, it would be of interest to use the Tg(*mpeg1*:dTomato), or another transgenic fluorescent macrophage zebrafish strain in order to visualize the macrophage response to IAV infection. If the neutrophil response is impaired, it may be possible that the innate immune system may try to compensate with other responding cells.

Assessing viral titer over a span of 96 hpi further supports the qualitative results of the confocal imaging. Control morphants had an increase of viral titer reach a maximum height of $9.04x10^7$ $TCID_{50}$/mL at 24 hpi (**Fig. 7A**). However, *ncf1* morphants only reached a maximum titer of $9.04x10^5$ $TCID_{50}$/mL at 48 hpi, a 1000-fold decrease compared to control morphants (**Fig. 7A**). Results were assessed by two individuals. Cytopathic effects were considered to be cell rounding, granularity, and grouping (**Figs. 7B, 7C, and 7D**). To increase the accuracy of result interpretation, it would be beneficial to have a third person interpret the results. Another replicate of the experiment must also be conducted in order for the results to be statistically significant, as only 2 were performed.

Finally, this study aimed to begin to characterize the gene expression of select anti-inflammatory and antiviral regulators in response to a *ncf1* knockdown. At 24 hpi, *ncf1* morphants have decreased expression of *nrf2*, *mxa*, and *cxcl8b* compared to controls during IAV infection (**Fig. 8**). This is as expected. Nuclear factor (erythroid-derived 2) 2 (Nrf2) is a key anti-inflammatory transcription factor in the innate immune system and has a direct relationship with Nox2 [33]. In order to combat the increase of ROS caused by the neutrophil antiviral response during IAV infection, Nrf2 would be normally be expressed at a high rate. The opposite seems to be true of the *ncf1* KD zebrafish model. Without a functional NADPH oxidase complex to produce ROS, Nrf2 and its downstream antioxidants would not be required to fight hyperinflammation. In this knockdown model, they would not be induced at the same rate as without the KD during infection.

Strikingly, *mxa*, an interferon-stimulated gene, is downregulated in the *ncf1* morphants (**Fig. 8**). Research has shown that in Ncf1 deficient humans and mice, type I interferon signaling increases [34]. Type I signaling is one of the main inducers of MxA expression in humans [35]. However, preliminary data from the Benjamin King lab at the University of Maine has shown that although *mxa* is initially upregulated in an *ncf1* KD zebrafish model of IAV infection, it quickly decreases after 6 hpi (Brandy Soos, unpublished). This data falls in line with these previous results, indicating that although there is an initial increase of type I signaling in the absence of *ncf1* during infection, it subsides by 24 hpi.

Interleukin 8 (IL-8) is encoded by the *cxcl8* gene and is an important chemokine attractant of neutrophils used for chemotaxis through the bloodstream [27]. Although the expression of *cxcl8b* is markedly increased compared to that of *nrf2* and *mxa*, it follows the same trend. This decrease in *cxcl8b* expression may be a contributing factor in the observed lowered neutrophil chemotaxis (**Fig. 8**). In the future, other CXC family genes associated with chemokine signaling should be investigated, such as *cxcl4b*.

All 3 genes of interest are expressed at roughly half of the level in *ncf1* morphants as they are in control morphants (**Fig. 8**), giving an initial insight into the genetic response to infection in this model. It is of interest to continue this aim by characterizing not only the first 24 hpi, but up to 96 hpi as well. Seeing the changes in gene expression over time would further serve to characterize the timeline of viral clearance in this KD model.

The improved survival and low viral burden of *ncf1* morphants are likely influenced by many different factors. The decrease of ROS production would not only

decrease the amount of host tissue damage at sites of infection, but also lead to a loss of signaling initiated by IAV upon infection. Without this ROS signaling, IAV may be unable to utilize the host's TLR7 signaling pathway to inhibit antiviral and antibody production. This should be confirmed in future studies by measuring downstream TLR7 signaling in the *ncf1* knockdown model. The phenotype could be further exacerbated by neutrophil modulation of other leukocytes. Macrophages are able to take on either pro-inflammatory or anti-inflammatory phases, known as "M1" and "M2" respectively. M1 macrophages will express an inducible nitric oxide synthase and produce signaling molecules such as TNF-α and IL-6 to protect against invading pathogens. M2 macrophages facilitate host tissue repair and produce TGF-β and IL-10 signaling molecules. During infection, neutrophils have been shown to induce the macrophage M1 phenotype for its pro-inflammatory response [36]. NOX2 has also been shown to drive M1-macrophage activity in a mouse model of neuroinflammation, while NOX2 inhibition increases IL-10 and anti-inflammatory signaling by macrophages [37, 38]. Although different than a zebrafish model of immunity, this data brings to question the contributions of neutrophil-modulated macrophage response during *ncf1* KD and IAV infection.

Chemical inhibition of NOX2 activity would be of interest in future study. Previous research has shown that diphenyleneiodonium (DPI) and VAS-2870 inhibition of NADPH oxidase activity blocks the suppression of $CD4^+$ effector T cells by regulatory T cells [39]. DPI has been shown to be able to inhibit NOX isoforms in a dose-dependent manner, making it ideal to test with IAV infection [40]. If able to produce similar results as

ncf1 MO, this would suggest DPI and possibly other drug NOX2 inhibitors for future therapeutic studies.

There are many facets of this project that should be subject to further scrutiny. Although a MO model is easily accessible, its effects only last about 7 dpf. Also, a KD only impairs gene expression, it does not completely inhibit it. Repeating these experiments with a CRISPR knockout model would be more effective in characterizing the effects on the innate immune system without Ncf1. Future experiments to enhance this characterization may include the measurement of ROS production using a neutrophil-specific respiratory burst assay, developed by the Kim lab at the University of Maine. Neutrophil migration should also be quantitatively analyzed to supplement the qualitative confocal imaging results. Further qRT-PCR should also be conducted, not only at the aforementioned time points but also for additional antioxidants, such as A1at and Sod1. Through this, more genetic targets may be identified for future therapies against IAV. Further research is needed to fully characterize the innate immune response to IAV in the absence of Ncf1 and provide targets for novel therapies for infection.

REFERENCES

1. World Health Organization (WHO). (2018). Influenza (Seasonal). Available at: https://www.who.int/news-room/fact-sheets/detail/influenza-(seasonal) [Accessed on September 21, 2019].

2. Fox, S.J., Miller, J.C., and Meyers, L.A. (2017). Seasonality in risk of pandemic influenza emergence. PLoS Comput. Biol. *13*, e1005749.

3. Shrestha, S.S., Swerdlow, D.L., Borse, R.H., Prabhu, V.S., Finelli, L., Atkins, C.Y., Owusu-Edusei, K., Bell, B., Mead, P.S., Biggerstaff, M., et al. (2011). Estimating the Burden of 2009 Pandemic Influenza A (H1N1) in the United States (April 2009-April 2010). Clin. Infect. Dis. *52*, S75–S82.

4. Sautto, G.A., Kirchenbaum, G.A., and Ross, T.M. (2018). Towards a universal influenza vaccine: Different approaches for one goal. Virol. J. *15*.

5. Hause, B.M., Collin, E.A., Liu, R., Huang, B., Sheng, Z., Lu, W., Wang, D., Nelson, E.A., and Li, F. (2014). Characterization of a novel influenza virus in cattle and swine: Proposal for a new genus in the Orthomyxoviridae family. MBio *5*.

6. Lofano, G., Kumar, A., Finco, O., Del Giudice, G., and Bertholet, S. (2015). B cells and functional antibody responses to combat influenza. Front. Immunol. *6*, 336.

7. WHO | Seasonal influenza. (2020).

8. Wilson, B.A. and Salyers, A.A. (2011). Bacterial Pathogenesis: A Molecular Approach. ASM, Print.

9. Mogensen, T. H. (2009). Pathogen recognition and inflammatory signaling in innate 32 immune defenses. Clin. Microbiol. Rev. *22*, 240–273.

10. Kobayashi, S.D., and DeLeo, F.R. (2009). Role of neutrophils in innate immunity: A systems biology-level approach. Wiley Interdisciplinary Reviews: Systems Biology and Medicine *1*, 309–333.

11. Brandes, M., Klauschen, F., Kuchen, S., and Germain, R.N. (2013). A systems analysis identifies a feedforward inflammatory circuit leading to lethal influenza infection. Cell *154*, 197-212.

12. Rada, B., Hably, C., Meczner, A., Timár, C., Lakatos, G., Enyedi, P., and Ligeti, E. (2008). Role of Nox2 in elimination of microorganisms. Semin. Immunopathol. *30*, 237–253.

13. Lam, G.Y., Huang, J., and Brumell, J.H. (2010). The many roles of NOX2 NADPH oxidase-derived ROS in immunity. Semin. Immunopathol. *32*, 415–430.

14. Mittal, M., Siddiqui, M.R., Tran, K., Reddy, S.P., Malik, A.B. (2014). Reactive Oxygen Species in Inflammation and Tissue Injury. Antioxid Redox Signal. *20(7)*, 1126–1167.

15. Nauseef, W.M. (2004). Assembly of the phagocyte NADPH oxidase. Histochem Cell Biol *122*, 277–291.

16. Mizuno, T., Kaibuchi, K., Ando, S., Musha, T., Hiraoka, K., Takaishi, K., Asada, M., Nunoi, H., Matsuda, I., and Takai, Y. (1992). Regulation of the superoxide-generating NADPH oxidase by a small GTP-binding protein and its stimulatory and inhibitory GDP/GTP exchange proteins. J. Biol. Chem. *267*, 10215–10218.

17. Brothers, K.M., Newman, Z.R., and Wheeler, R.T. (2011). Live imaging of disseminated candidiasis in zebrafish reveals role of phagocyte oxidase in limiting filamentous growth. Eukaryot. Cell *10*, 932–944.

18. Ha Kim, K., Sadikot, R.T., Yeon Lee, J., Jeong, H.S., Oh, Y.K., Blackwell, T.S., and Joo, M. (2017). Suppressed ubiquitination of Nrf2 by p47phox contributes to Nrf2 activation. Free Radic. Biol. Med. *113*, 48–58.

19. Lieschke, G.J., and Currie, P.D. (2007). Animal models of human disease: Zebrafish swim into view. Nat. Rev. Genet. *8*, 353–367.

20. Goldsmith, J.R., and Jobin, C. (2012). Think Small: Zebrafish as a Model System of Human Pathology. Journal of Biomedicine and Biotechnology *2012*, 1-12.

21. Gabor, K.A., Goody, M.F., Mowel, W.K., Breitbach, M.E., Gratacap, R.L., Witten, P.E., and Kim, C.H. (2014). Influenza A virus infection in zebrafish recapitulates mammalian infection and sensitivity to anti-influenza drug treatment. Dis. Model. Mech. *7*, 1227–1237.

22. Bouvier, N.M., and Lowen, A.C. (2010). Animal Models for Influenza Virus Pathogenesis and Transmission. Viruses *2*, 1530-1563.

23. Westerfield, M. (2000). The zebrafish book: A guide for the laboratory use of zebrafish (Danio rerio) Oregon Press. *4*.

24. Fukuyama, S., Katsura, H., Zhao, D., Ozawa, M., Ando, T., Shoemaker, J.E., Ishikawa, I., Yamada, S., Neumann, G., Watanabe, S., et al. (2015). Multi-spectral fluorescent reporter influenza viruses (Color-flu) as powerful tools for in vivo studies. Nat. Commun. *6*, 1–8.

25. Robu, M.E., Larson, J.D., Nasevicius, A., Beiraghi, S., Brenner, C., Farber, S.A., and Ekker, S.C. (2007). p53 Activation by Knockdown Technologies. PLoS Genet. *3*, e78.

26. Ma, Q. (2013). Role of Nrf2 in Oxidative Stress and Toxicity. Annu. Rev. Pharmacol. Toxicol. *53*, 401–426.

27. Zuñiga-Traslaviña, C., Bravo, K., Reyes, A.E., and Feijóo, C.G. (2017). Cxcl8b and Cxcr2 Regulate Neutrophil Migration through Bloodstream in Zebrafish. J Immunol Res. *2017*, 6530531.

28. Grandvaux, N., Mariani, M., and Fink, K. (2015). Lung Epithelial NOX/DUOX and Respiratory Virus Infections. Clin. Sci. Clinical Science *128.6*, 337-47.

29. Vowells, S.J., Fleisher, T.A., Sekhsaria, S., Alling, D.W., Maguire, T.E., Malech, H.L. (1996). Genotype-dependent variability in flow cytometric evaluation of reduced nicotinamide adenine dinucleotide phosphate oxidase function in patients with chronic granulomatous disease. J. Pediatr. *128*, 104–107.

30. Kuhns, D.B., Alvord, W.G., Heller, T., Feld, J.J., Pike, K.M., Marciano, B.E., Uzel, G., DeRavin, S.S., Priel, D.A.L., Soule, B.P., Zarember, K.A., Malech, H.L., Holland, S.M., Gallin, J.I. (2010). Residual NADPH oxidase and survival in chronic granulomatous disease. N. Engl. J. Med. *363*, 2600–2610.

31. To, E.E., Vlahos, R., Luong, R., Halls, M.L., Reading, P.C., King, P.T., Chan, C., Drummond, G.R., Sobey, C.G., Broughton, B.R.S., et al. (2017). Endosomal NOX2 oxidase exacerbates virus pathogenicity and is a target for antiviral therapy. Nat. Commun. *8*.

32. Langheinrich, U., Hennen, E., Stott, G., and Vacun, G. (2002). Zebrafish as a model organism for the identification and characterization of drugs and genes affecting p53 signaling. Curr. Biol. *12*, 2023–2028.

33. Kovac, S., Angelova, P.R., Holmström, K.M., Zhang, Y., Dinkova-Kostova, A.T., and Abramov, A.Y. (2015). Nrf2 regulates ROS production by mitochondria and NADPH oxidase. Biochim. Biophys. Acta - Gen. Subj. *1850*, 794–801.

34. Kelkka, T., Kienhöfer, D., Hoffmann, M., Linja, M., Wing, K., Sareila, O., Hultqvist, M., Laajala, E., Chen, Z., Vasconcelos, J., et al. (2014). Reactive oxygen species deficiency induces autoimmunity with type 1 interferon signature. Antioxidants Redox Signal. *21*, 2231–2245.

35. Holzinger, D., Jorns, C., Stertz, S., Boisson-Dupuis, S., Thimme, R., Weidmann, M., Casanova, J.-L., Haller, O., and Kochs, G. (2007). Induction of MxA Gene Expression by Influenza A Virus Requires Type I or Type III Interferon Signaling. J. Virol. *81*, 7776–7785.

36. Prame Kumar, K., Nicholls, A.J., and Wong, C.H.Y. (2018). Partners in crime: neutrophils and monocytes/macrophages in inflammation and disease. Cell Tissue Res. *371*, 551–565.

37. Kumar, A., Barrett, J.P., Alvarez-Croda, D.M., Stoica, B.A., Faden, A.I., and Loane, D.J. (2016). NOX2 drives M1-like microglial/macrophage activation and neurodegeneration following experimental traumatic brain injury. Brain. Behav. Immun. *58*, 291–309.

38. Barrett, J.P., Henry, R.J., Villapol, S., Stoica, B.A., Kumar, A., Burns, M.P., Faden, A.I., and Loane, D.J. (2017). NOX2 deficiency alters macrophage phenotype through an IL-10/STAT3 dependent mechanism: Implications for traumatic brain injury. J. Neuroinflammation *14*, 65.

39. Efimova, O., Szankasi, P., and Kelley, T.W. (2011). Ncf1 (p47phox) is essential for direct regulatory T cell mediated suppression of CD4+ effector T cells. PLoS One *6*, e16013.

40. Augsburger, F., Filippova, A., Rasti, D., Seredenina, T., Lam, M., Maghzal, G., Mahiout, Z., Jansen-Dürr, P., Knaus, U.G., Doroshow, J., et al. (2019). Pharmacological characterization of the seven human NOX isoforms and their inhibitors. Redox Biol. *26*.

AUTHOR'S BIOGRAPHY

Lily Charpentier was raised in Naples, ME and graduated Lake Region High School in 2016. She is majoring in biochemistry and plans to pursue a Ph.D. in molecular and cellular biology once she graduates from the University of Maine. Lily enjoys spending time with her family and creating art.